Formulas for Beam Shift and Beam Narrowing in 1-D Leaky-Wave Antennas Due to Element Pattern

Walter Fuscaldo, *Senior Member, IEEE*, Alessandro Galli, *Member, IEEE*, and David R. Jackson, *Fellow, IEEE*

***Abstract*—The radiation pattern of 1-D unidirectional leaky-wave antennas (LWAs) is typically derived from the analysis of the *space factor* (SF) only. However, when the antenna aperture is characterized by a longitudinal radiating current, a cosine-type *element pattern* term has to be included: this factor may considerably affect the beam properties. Specifically, the beam peak is shifted and the beamwidth is narrowed when the element pattern is included. These effects are more prominent as the antenna size decreases and the beam angle increases. Approximate but accurate analytical formulas are here provided and numerically validated to predict the beam angle and the half-power beamwidth for these kinds of 1-D unidirectional LWAs when the element pattern is included.**

***Index Terms*—Antenna radiation patterns, antenna theory, beamwidth, leaky waves, leaky-wave antennas.**

I. Introduction

RECENT progress has been made to improve the estimation of the beam angle θ_0 and the half-power beamwidth Θ_h in 1-D leaky-wave antennas (LWAs) for both unidirectional [1], [2], [3], [4], [5], [6] and bidirectional excitations [7], [8], [9]. Most of these works provided corrections to the asymptotic formulas derived in [10] and [11], when the antenna is truncated, but assume that the radiation pattern is based solely on the space factor (SF). This assumption holds when the antenna aperture is characterized by a transverse radiating current (see Fig. 1, top), as in LWAs with transverse slots [12], [13], [14]. When the antenna aperture is characterized by a longitudinal radiating current (see Fig. 1, bottom), as in slitted waveguide LWAs [15], the SF has to be multiplied by a $\cos\theta$ factor (θ being measured from the vertical z-axis) that accounts for the dipole-like element pattern. This can be described as a *polarization effect*, as it depends on the polarization of the current.

The work in [5] originally investigated this problem in detail, showing that when the beam peak approaches endfire ($\theta_0 \to 90°$) and for electrically short antenna lengths ($L \ll 10\,\lambda_0$), this aspect has nonnegligible effects on the radiation pattern: *i)* the *actual* beam angle $\theta_{0\mathrm{p}}$ is *shifted* with respect to that predicted from the SF only, viz., θ_0; *ii)* the *actual* beamwidth Θ_{hp} (measured between the -3 dB points) is narrowed with respect to that predicted from the SF only, viz., Θ_h. These *polarization effects* are a consequence of the null at endfire enforced by the cosine term.

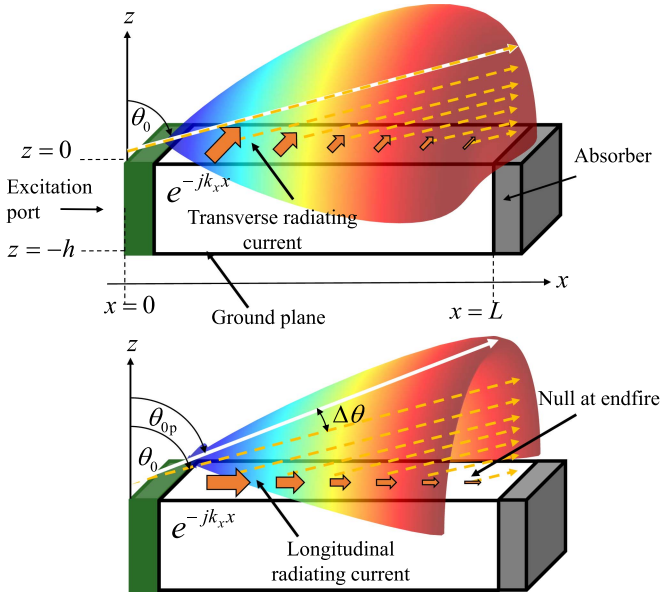

Fig. 1. 1-D unidirectional LWA of length L terminated with an ideal absorber, radiating a scanned beam. A null at endfire is due to the element pattern of a longitudinal current (bottom), which is absent for a transverse current (top). Dashed orange lines point in the direction of leakage, whereas solid white lines point to the beam maximum (θ_0 in the top figure, $\theta_{0\mathrm{p}}$ in the bottom figure).

The investigation in [5] reported numerical results for some specific cases and an experimental validation, without providing any formulas to predict the observed beam shift and the beam narrowing. Here, we propose approximate, fully analytical formulas to accurately predict both the beam angle and the beamwidth in 1-D unidirectional LWAs accounting for the polarization effect. In this regard, we should stress that the formulas proposed in [6] for 1-D unidirectional LWAs, although including the element pattern, assumed the cosine term be approximately constant near the beam peak, and therefore ignored its effect. As a result, the formula in [6, eq. (20)] is almost equivalent to the one later proposed in [3, eq. (6)], which indeed ignores polarization effects.

This letter is organized as follows. Section II describes the problem and motivates the need for the formulas. In Section III, analytical formulas are derived for both the beam angle and the beamwidth, and then validated with numerical results. Conclusions are finally drawn in Section IV.

Manuscript received 24 February 2023; accepted 14 March 2023. Date of publication 20 March 2023; date of current version 7 July 2023. *(Corresponding author: Walter Fuscaldo.)*

Walter Fuscaldo is with the Consiglio Nazionale delle Ricerche, Istituto per la Microelettronica e Microstistemi, 00133 Rome, Italy (e-mail: walter.fuscaldo@cnr.it).

Alessandro Galli is with the Department of Information Engineering, Electronics and Telecommunications, Sapienza University of Rome, 00184 Rome, Italy (e-mail: alessandro.galli@uniroma1.it).

David R. Jackson is with the Department of Electrical and Computer Engineering, University of Houston, Houston, TX 77204-4005 USA (e-mail: djackson@uh.edu).

Digital Object Identifier 10.1109/LAWP.2023.3259743

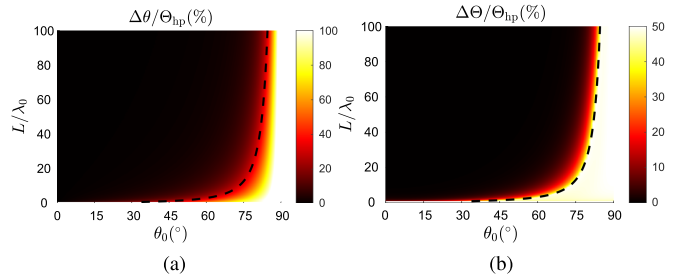

Fig. 2. (a) Beam shift normalized with respect to the half-power beamwidth versus θ_0 and L/λ_0. (b) As in (a) but showing the normalized change in the beamwidth. The dashed black curve shows the "discontinuity angle" $\theta_{0\mathrm{d}}$ for the SF pattern (the far-field pattern without the element pattern included).

II. Description of the Problem

The reference structure is the one reported in Fig. 1 and consisting of a 1-D unidirectional LWA of length L, whose radiating aperture is dominated by a single leaky mode characterized by a complex leaky wavenumber $k_x = \beta - j\alpha$. In this case, the SF is obtained by Fourier-transforming the radiating current distribution, which reads $\exp(-jk_x x)\Pi(x/L - 0.5)$, where $\Pi(\cdot)$ is the centered unit rectangular pulse. When a transverse radiating current is assumed, the radiation power pattern is obtained by just taking the modulus squared of the SF and thus reads [1]

$$P_0(\theta) := |\mathrm{SF}|^2 = \left(\sin^2 t + \sinh^2 a\right) / \left(t^2 + a^2\right) \tag{1}$$

where we have conveniently defined the normalized variables $t = b - l\sin\theta$ and $a = \hat{\alpha} l$, with $b = \hat{\beta} l$ and $l = \pi L/\lambda_0$, and the normalized phase $\hat{\beta} := \beta/k_0$ and attenuation $\hat{\alpha} := \alpha/k_0$ constants, $k_0 = 2\pi/\lambda_0$ being the free-space wavenumber.

When a longitudinal radiating current is assumed, the SF has to be multiplied by a cosine term, and thus the radiation power pattern reads

$$P(\theta) = P_0(\theta)\cos^2\theta. \tag{2}$$

From these two expressions, it is possible to numerically evaluate the beam angles and the half-power beamwidths. The results are reported in Fig. 2(a) and (b), where the deviations of the beam angles (namely, the *beam shift*) and the beamwidths, defined as $\Delta\theta = \theta_0 - \theta_{0\mathrm{p}}$, and $\Delta\Theta = \Theta_\mathrm{h} - \Theta_\mathrm{hp}$ are both normalized to the half-power beamwidth Θ_hp (and then multiplied by 100 to get percent) and shown as functions of L and θ_0 to highlight how important the beam shift and the change in the beamwidth really are. This normalization is relevant to highlight the practical importance of the changes in the beam angle and the beamwidth.

In both cases, the radiation efficiency $e_\mathrm{r} = 1 - \exp(-4a)$ is fixed to 20% (this choice will be further motivated next), and hence the leakage rate is in the range $10^{-4} \le \hat{\alpha} \le 10^{-2}$ for $1 \le L/\lambda_0 \le 100$, which is rather practical. Results do not substantially change as long as $e_\mathrm{r} < 0.99$ (for $e_\mathrm{r} > 0.99$ and $L < 5\,\lambda_0$, then $\hat{\alpha} > 0.1$ and the leaky mode might no longer be dominant [10], [11], thus controverting the initial assumption).

The results in Fig. 2(a) and (b) clearly highlight that polarization effects are negligible for $\theta_0 < 45°$ regardless of the antenna size, whereas they are increasingly more appreciable for $\theta_0 > 45°$ and more so as θ_0 increases and L/λ_0 decreases. The boundary between these two regions is reported as a black dashed line in Fig. 2(a) and (b). Remarkably, this boundary can be predicted by the following formula for the "discontinuity angle" $\theta_{0\mathrm{d}} = \arcsin(1 - t_\mathrm{h}/l)$ discussed in [3], where $t_\mathrm{h} = 1.39156[1 - \tanh(0.021a)] + a\tanh(0.21a)$. This formula gives the beam angle θ_0 for which the right-sided -3 dB point would be at endfire, ignoring polarization effects. As can be inferred from Fig. 2(a) and (b), polarization effects become important for $\theta_0 > \theta_{0\mathrm{d}}$.

We note that the results reported so far are consistent with those obtained in [5] for a limited number of cases. Moreover, they clearly show that polarization effects cannot be neglected for practical LWAs radiating close to endfire, thus motivating the interest in having analytical formulas for a correct prediction of both the beam angle and the beamwidth. The following Section III is thus devoted to this task.

III. Analytical Formulas

A. Beam Shift

We start by deriving a formula for correctly predicting the beam angle from the expression for $P(\theta)$ in (2). A straightforward application of the first derivative test to find the local maximum does not allow for a closed-form solution, thus we first use the following "key" approximation for $P_0(\theta)$:

$$P_0(\theta) = 1 - (t/t_\mathrm{h})^2/2 \tag{3}$$

which is obtained from (2) by means of a second-order Taylor expansion with respect to t and near θ_0 (for which $t = 0$), which is the exact beam peak for P_0. Note that $t = \pm t_\mathrm{h}$ corresponds to the left/right -3 dB points of P_0. By exploiting the definition of t, and using (3), (2) can be recast as a function of t only

$$P(t) = \left[1 - \left(\frac{b-t}{l}\right)^2\right]\left(1 - \frac{1}{2}\frac{t^2}{t_\mathrm{h}^2}\right). \tag{4}$$

The application of the first derivative test to this expression with respect to the variable t leads to a cubic polynomial equation $a_3 t^3 + a_2 t^2 + a_1 t + a_0 = 0$ whose coefficients have the following expressions:

$$\begin{aligned} a_3 &= 2/(lt_\mathrm{h})^2 & a_2 &= -3b/(lt_\mathrm{h})^2 \\ a_1 &= b^2/(t_\mathrm{h} l)^2 - 1/t_\mathrm{h}^2 - 2/l^2 & a_0 &= 2b/l^2. \end{aligned} \tag{5}$$

Although there exist three roots, Descartes' signs rule tells us that there exist only two positive roots, but does not provide any guess about which one should be the correct one. With the help of numerical calculations and the use of Cardano's formula, it is found that the correct root in t is given by

$$t_\mathrm{p} = -\left(a_2 + C + \Delta_0/C\right)/(3a_3) \tag{6}$$

where

$$C = e^{j2\pi/3}\left[\left(\Delta_1 - \sqrt{\Delta_1^2 - 4\Delta_0^3}\right)/2\right]^{1/3} \tag{7}$$

with $\Delta_0 = a_2^2 - 3a_3 a_1$ and $\Delta_1 = 2a_2^3 - 9a_3 a_2 a_1 + 27a_3^2 a_0$ and where the cubic and square roots are interpreted as the principal branches. The beam angle is finally found by using the definition of t, which yields

$$\theta_{0\mathrm{p}} = \arcsin(\hat{\beta} - t_\mathrm{p}/l). \tag{8}$$

The accuracy of (6) and (8) can be inferred from Fig. 3(a), where numerical results for the SF only (solid line) and for

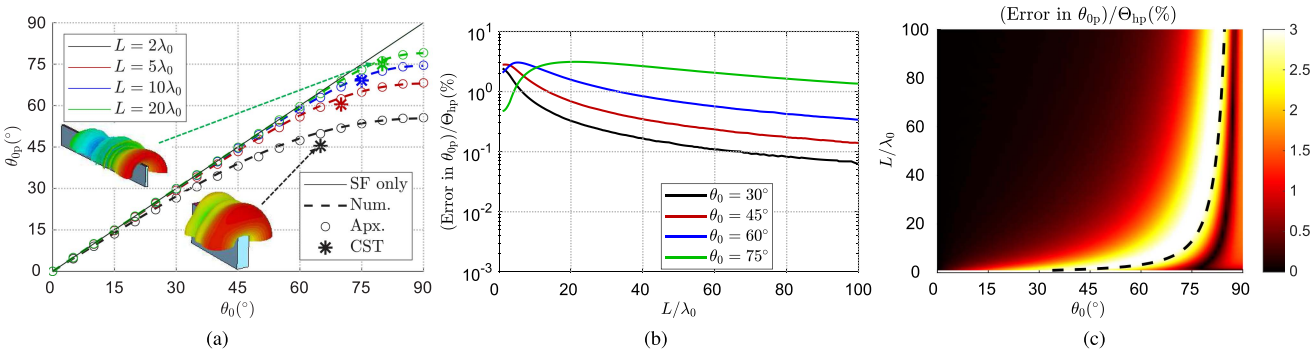

Fig. 3. (a) Beam angle versus θ_0 for different lengths. (b) Normalized error in the new beam angle formula (normalized to the beamwidth), expressed in percent. Results are shown versus L/λ_0 for various beam angles θ_0. (c) 2-D error map showing the normalized error in the new beam angle formula versus θ_0 and L/λ_0. The dashed black curve shows the "discontinuity angle" θ_{0d}. The insets in (a) show the 3-D radiation patterns of two practical LWAs of length $L = 2\,\lambda_0$ and $L = 20\,\lambda_0$ as simulated in CST.

the polarization effect (dashed lines) are compared with those given by the analytical formula (circles) for different antenna lengths when θ_0 is allowed to vary from broadside to endfire. The formula is remarkably accurate as confirmed also by Fig. 3(b) and (c), where its error relative to the beamwidth is seen to be under a few percent.

For a few cases CST full-wave validations have been performed. Namely, we considered four different LWAs based on rectangular waveguides operating at $f_0 = 10$ GHz in their fundamental TE mode and with one of the side walls replaced by a PRS to allow for radiation. The simulation setup is based on the *ideal* model of 1-D PRS-based LWAs described in [16, Sec. V.A], which is not elaborated on here for the sake of brevity. As opposed to the examples discussed in [16] that are optimized for maximum gain, here the structures are designed with a rather low radiation efficiency, viz., 20%, to accentuate the effects of the element pattern and, at the same time, have a practical value of $\hat{\alpha}$ with a short antenna.

For a fixed radiation efficiency of 20%, we thus designed four different antennas radiating at $\theta_0 = 65^\circ$, 70°, 75°, 80° when $L/\lambda_0 = 2$, 5, 10, 20, respectively, using the equations provided in [16, Sec. V(a)]. The angles of maximum radiation are then extracted from the simulated, full-wave 3-D radiation patterns and reported as colored asterisks in Fig. 3(a). In all cases, an overall good agreement is obtained.

B. Beamwidth

The derivation of the beamwidth formula is based on the same approximation used for the beam shift in the previous Section III-A. In addition, the first term in square brackets in (4) is further expanded with a Taylor series at $t = 0$. Depending on whether a first- or a second-order expansion is used, a third-order or a fourth-order polynomial equation is obtained as we will discuss later.

In order to obtain a beamwidth equation, the power pattern is usually normalized to its maximum and then equated to a half. Here, the pattern is first normalized with respect to its value at $t = 0$ (which is equal to $\cos^2\theta_0$), which is not exactly where the maximum occurs due to the element pattern. The normalized pattern is then equated not to a half, but to half the value of the normalized pattern at $t = t_\mathrm{p}$ [which is now known from (6)].

The expressions of the coefficients of the third-order polynomial equation $b_3 t^3 + b_2 t^2 + b_1 t + b_0 = 0$ obtained from a first-order Taylor expansion are as follows:

$$b_3 = -\sec\theta_0 \tan\theta_0/(l t_\mathrm{h}^2) \qquad b_2 = -1/(2t_h^2)$$
$$b_1 = 2\sec\theta_0 \tan\theta_0/l \qquad b_0 = 1 - P_\mathrm{m}^{(1)}/2 \tag{9}$$

whereas those of the fourth-order polynomial equation $c_4 t^4 + c_3 t^3 + c_2 t^2 + c_1 t + c_0 = 0$ obtained from a second-order Taylor expansion are as follows:

$$c_4 = \sec^2\theta_0/(2\,l^2 t_\mathrm{h}^2) \qquad c_3 = -\sec\theta_0 \tan\theta_0/(l t_\mathrm{h}^2)$$
$$c_2 = -1/(2t_\mathrm{h}^2) - \sec^2\theta_0/l^2 \qquad c_1 = 2\sec\theta_0 \tan\theta_0/l$$
$$c_0 = 1 - P_\mathrm{m}^{(2)}/2 \tag{10}$$

with

$$P_\mathrm{m}^{(1)} = \left(1 + \frac{2\sin\theta_0}{l\cos^2\theta_0} t_\mathrm{p}\right)\left(1 - \frac{t_\mathrm{p}^2}{2t_\mathrm{h}^2}\right) \tag{11}$$

$$P_\mathrm{m}^{(2)} = \left(1 + \frac{2\sin\theta_0}{l\cos^2\theta_0} t_\mathrm{p} - \frac{\sec^2\theta_0}{l^2} t_\mathrm{p}^2\right)\left(1 - \frac{t_\mathrm{p}^2}{2t_\mathrm{h}^2}\right) \tag{12}$$

where $P_\mathrm{m}^{(1)}$ and $P_\mathrm{m}^{(2)}$ are the normalized power patterns evaluated at $t = t_\mathrm{p}$ and obtained after a first-order and a second-order Taylor expansion, respectively. (The reason why we keep both approximations will be soon clarified.)

Following the discussion in [3], the expression of the beamwidth of a 1-D unidirectional LWA when polarization effects are accounted for can be expressed as

$$\Theta_\mathrm{hp} = \arcsin\left(\hat{\beta} - t_\mathrm{hp}^\mathrm{r}/l\right) - \arcsin\left(\hat{\beta} - t_\mathrm{hp}^\mathrm{l}/l\right) \tag{13}$$

where $t_\mathrm{hp}^\mathrm{r} < 0$ and $t_\mathrm{hp}^\mathrm{l} > 0$ notably refer to the right and left -3 dB points, respectively (note that in [3, eq. (6)] only the SF is taken into account and thus $t_\mathrm{hp}^\mathrm{r} = -t_\mathrm{hp}^\mathrm{l} = -t_\mathrm{h}$). However, from Descartes' signs rule we can expect at least two positive roots in both cases from (9) and (10). A criterion is thus needed for choosing the correct determination.

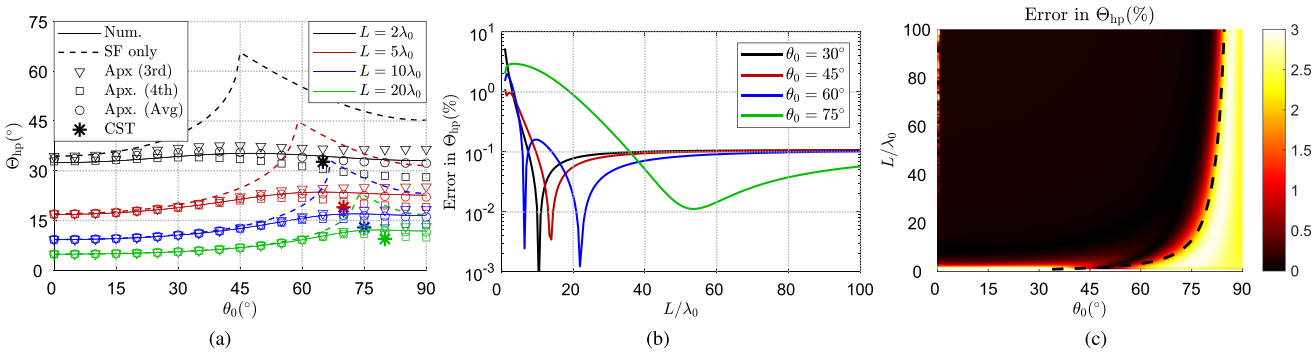

Fig. 4. (a) $\Theta_{\rm hp}$ versus θ_0 for different lengths. (b) Percent error in $\Theta_{\rm hp}$ versus L/λ_0 for different beam angles. (c) 2-D error map of $\Theta_{\rm hp}$ versus θ_0 and L/λ_0. The dashed black line shows the "discontinuity angle" $\theta_{0\rm d}$.

For the third-order polynomial equation, we found that one can use (6) as is (obviously replacing the coefficients a_i with b_i, $\forall i$). However, one should be careful with the root definition for C in (7): for $t_{\rm hp}^{\rm r}$ the expression for C is the same as in (7), whereas for $t_{\rm hp}^{\rm l}$ the expression for C in (7) should be multiplied by $e^{-j2\pi/3}$ to get the correct root.

For the fourth-order polynomial equation, one has to resort to Ferrari–Cardano's formulas. Among the four possible roots, the two correct choices are

$$t_{\rm hp}^{\rm r} = -c_3/(4c_4) - S + (1/2)\sqrt{-4S^2 - 2p + q/S} \quad (14)$$

$$t_{\rm hp}^{\rm l} = -c_3/(4c_4) + S - (1/2)\sqrt{-4S^2 - 2p + q/S} \quad (15)$$

with $p = (8c_4c_2 - 3c_3^2)/(8c_4^2)$, $q = (c_3^3 - 4c_4c_3c_2 + 8c_4^2c_1)/(8c_4^3)$, and the known expressions for S and Q read

$$S = \frac{1}{2}\sqrt{\frac{-2p}{3} + \frac{1}{3c_4}\left(Q + \frac{\Delta_0'}{Q}\right)} \quad (16)$$

$$Q = \left(\frac{\Delta_1' + \sqrt{(\Delta_1')^2 - 4(\Delta_0')^3}}{2}\right)^{1/3} \quad (17)$$

with $\Delta_0' = c_2^2 - 3c_3c_1 + 12c_0c_4$, and $\Delta_1' = 2c_2^3 - 9c_3c_2c_1 + 27c_3^2c_0 + 27c_4c_1^2 - 72c_4c_2c_0$.

The accuracy of the beamwidth formula with the third-order and the fourth-order polynomial expressions can be inferred from Fig. 4(a) where they are reported as triangles and squares, respectively. Notably, the third-order polynomial provides a slight overestimation, whereas the fourth-order polynomial provides a slight underestimation. The average between the values provided by these two expressions (in circles) turns out to be an excellent estimation of the beamwidth. For comparison purposes, the beamwidth as predicted by the SF only is also reported (dashed lines), showing that polarization effects considerably affect the beamwidth as the beam peak increases beyond 45°, especially for short antenna sizes. The accuracy of the formula obtained as the average value of the third-order and fourth-order polynomial expressions is further highlighted by the error plots in Fig. 4(b) and (c), where the error is shown to be at most a few percent. As per the beam shift, full-wave results from the same examples of Section III-A are reported with colored asterisks, showing very good agreement.

TABLE I
BEAM ANGLES AND BEAMWIDTHS FOR $L/\lambda_0 = 20$ AND $e_{\rm r} = 92\%$

		Beam Angle θ_0			
Beam Property	Method	$\theta_0 = 30^\circ$	$\theta_0 = 45^\circ$	$\theta_0 = 60^\circ$	$\theta_0 = 75^\circ$
$\theta_{0\rm p}$	Num.	29.9640	44.9065	59.6833	73.0941
	This work	29.9528	44.8781	59.5929	72.8194
$\Delta\theta/\Theta_{\rm hp}$	Num.	0.0117	0.0249	0.0605	0.2281
	This work	0.0153	0.0325	0.0778	0.2609
$\Theta_{\rm hp}/\Theta_{\rm h}$	Num.	0.9988	0.9960	0.9795	0.7564
	This work	0.9967	0.9941	0.9780	0.7431

For the sake of completeness, Table I also reports some numerical values for a few practical cases of a LWA of 20 λ_0 with a radiation efficiency of about 92%, which is approximately the value required to have optimum gain [3].

Table I shows that for a moderately large LWA length ($L = 20\,\lambda_0$), the effects of the element pattern on the beam shift and the beamwidth are only significant when the beam is scanned past about 75°. At 75°, the beam shift due to the element pattern is about 23% of the beamwidth, and the element pattern has also caused the beam to have narrowed to about 76% of that predicted by the SF alone. We should note that neither the formula in [3] nor that in [6] are capable of predicting the beam narrowing effect, although the radiation power pattern in [6] includes the element pattern (whereas [3] does not).

IV. Conclusion

The effects of the element pattern in 1-D unidirectional LWAs is demonstrated to be important when the beam angle approaches endfire and the antenna size is short. Approximate, accurate, fully analytical formulas are derived here for correctly estimating both the beam angle and the beamwidth when the element pattern is included. Although derived for an untapered aperture, the formulas are also accurate for apertures having a fairly gradual taper (results not shown for brevity). Previous formulas, based on the SF only, are instead shown to be no longer accurate when the beam angle approaches endfire; a criterion to determine the region where the formula loses accuracy is also provided. Results are extensively validated numerically to verify the accuracy of the new formulas.

REFERENCES

[1] W. Fuscaldo, D. R. Jackson, and A. Galli, "A general and accurate formula for the beamwidth of 1-D leaky-wave antennas," *IEEE Trans. Antennas Propag.*, vol. 65, no. 4, pp. 1670–1679, Apr. 2017.

[2] W. Fuscaldo, D. R. Jackson, and A. Galli, "Beamwidth properties of endfire 1-D leaky-wave antennas," *IEEE Trans. Antennas Propag.*, vol. 65, no. 11, pp. 6120–6125, Nov. 2017.

[3] W. Fuscaldo, A. Galli, and D. R. Jackson, "Optimization of the radiating features of 1-D unidirectional leaky-wave antennas," *IEEE Trans. Antennas Propag.*, vol. 70, no. 1, pp. 111–125, Jan. 2022.

[4] D. Xie and L. Zhu, "Effective approach to reduce variation of quasi-E-plane beamwidth of EH_1-mode microstrip leaky-wave antennas," *IEEE Antennas Wireless Propag. Lett.*, vol. 17, no. 9, pp. 1732–1735, Sep. 2018.

[5] M. Schühler, R. Wansch, and M. A. Hein, "On strongly truncated leaky-wave antennas based on periodically loaded transmission lines," *IEEE Trans. Antennas Propag.*, vol. 58, no. 11, pp. 3505–3514, Nov. 2010.

[6] I. Bahl and K. Gupta, "A leaky-wave antenna using an artificial dielectric medium," *IEEE Trans. Antennas Propag.*, vol. 22, no. 1, pp. 119–122, Jan. 1974.

[7] A. Sutinjo, M. Okoniewski, and R. H. Johnston, "Beam-splitting condition in a broadside symmetric leaky-wave antenna of finite length," *IEEE Antennas Wireless Propag. Lett.*, vol. 7, no. 7, pp. 609–612, Jul. 2008.

[8] G. Lovat, P. Burghignoli, and D. R. Jackson, "Fundamental properties and optimization of broadside radiation from uniform leaky-wave antennas," *IEEE Trans. Antennas Propag.*, vol. 54, no. 5, pp. 1442–1452, May 2006.

[9] W. Fuscaldo, D. R. Jackson, and A. Galli, "General formulas for the beam properties of 1-D bidirectional leaky-wave antennas," *IEEE Trans. Antennas Propag.*, vol. 67, no. 6, pp. 3597–3608, Jun. 2019.

[10] T. Tamir and A. A. Oliner, "Guided complex waves. Part 1: Fields at an interface," *Proc. IEE*, vol. 110, no. 2, pp. 310–324, Feb. 1963.

[11] T. Tamir and A. A. Oliner, "Guided complex waves. part 2: Relation to radiation patterns," *Proc. IEE*, vol. 110, no. 2, pp. 325–334, Feb. 1963.

[12] J. Liu, D. R. Jackson, and Y. Long, "Substrate integrated waveguide (SIW) leaky-wave antenna with transverse slots," *IEEE Trans. Antennas Propag.*, vol. 60, no. 1, pp. 20–29, Jan. 2012.

[13] J. Liu, D. R. Jackson, Y. Li, C. Zhang, and Y. Long, "Investigations of SIW leaky-wave antenna for endfire-radiation with narrow beam and sidelobe suppression," *IEEE Trans. Antennas Propag.*, vol. 62, no. 9, pp. 4489–4497, Sep. 2014.

[14] E. M. O'Connor, D. R. Jackson, and S. A. Long, "Extension of the Hansen-Woodyard condition for endfire leaky-wave antennas," *IEEE Antennas Wireless Propag. Lett.*, vol. 9, no. 11, pp. 1201–1204, Nov. 2010.

[15] L. Goldstone and A. A. Oliner, "Leaky-wave antennas I: Rectangular waveguides," *IRE Trans. Antennas Propag.*, vol. 7, no. 4, pp. 307–319, Oct. 1959.

[16] W. Fuscaldo, A. Galli, and D. R. Jackson, "Optimization of 1-D unidirectional leaky-wave antennas based on partially reflecting sheets," *IEEE Trans. Antennas Propag.*, vol. 70, no. 9, pp. 7853–7868, Sep. 2022.

Open Access provided by 'Consiglio Nazionale delle Ricerche-CARI-CARE' within the CRUI CARE Agreement